INL/CON-21-62801-Revision-0

Conceptual Design of Temperature-Controlled Fueled-Salt Irradiation Experiment to Support Demonstration of Advanced Nuclear Reactors

November 2021

Abdalla Abou Jaoude, Gregory M Core, William C Phillips, Kim B Davies, Calvin Myer Downey, Stacey M Wilson, Chuting Tan, James Loren Chandler

Changing the World's Energy Future

INL is a U.S. Department of Energy National Laboratory operated by Battelle Energy Alliance, LLC

DISCLAIMER

This information was prepared as an account of work sponsored by an agency of the U.S. Government. Neither the U.S. Government nor any agency thereof, nor any of their employees, makes any warranty, expressed or implied, or assumes any legal liability or responsibility for the accuracy, completeness, or usefulness, of any information, apparatus, product, or process disclosed, or represents that its use would not infringe privately owned rights. References herein to any specific commercial product, process, or service by trade name, trade mark, manufacturer, or otherwise, does not necessarily constitute or imply its endorsement, recommendation, or favoring by the U.S. Government or any agency thereof. The views and opinions of authors expressed herein do not necessarily state or reflect those of the U.S. Government or any agency thereof.

INL/CON-21-62801-Revision-0

Conceptual Design of Temperature-Controlled Fueled-Salt Irradiation Experiment to Support Demonstration of Advanced Nuclear Reactors

Abdalla Abou Jaoude, Gregory M Core, William C Phillips, Kim B Davies, Calvin Myer Downey, Stacey M Wilson, Chuting Tan, James Loren Chandler

November 2021

Idaho National Laboratory
Idaho Falls, Idaho 83415

http://www.inl.gov

Prepared for the
U.S. Department of Energy
Under DOE Idaho Operations Office
Contract DE-AC07-05ID14517

Proceedings of the ASME 2021
International Mechanical Engineering Congress and Exposition
IMECE2021
November 1-5, 2021, Virtual, Online

IMECE2021-69204

CONCEPTUAL DESIGN OF TEMPERATURE-CONTROLLED FUELED-SALT IRRADIATION EXPERIMENT TO SUPPORT DEMONSTRATION OF ADVANCED NUCLEAR REACTORS

Abdalla Abou-Jaoude[1], James Chandler[1], Gregory Core[1], Kim Davies[1], Calvin Downey[1], William Phillips[1], and Chuting Tan[1], and Stacey Wilson[1]
[1]Idaho National Laboratory
Idaho Falls, ID

ABSTRACT

Irradiation testing of fuel-bearing molten salts is critical for supporting the development and demonstration of molten salt reactors (MSRs). These experiments can inform several important reactor design and safety parameters, including source term modeling, the evolution of thermophysical properties with burnup, and the degradation of structural materials under reactor-relevant conditions. Idaho National Laboratory is designing an instrumented and heated high-temperature molten-salt-fueled irradiation capsule to study the behavior of the fuel salt during in-pile irradiation. This paper details the neutronics, thermal, and mechanical analyses performed to date. Parametric studies were performed to assess a range of materials, different experiment dimensions, two in-reactor positions, and the fuel enrichment used. The principal recommendations are to select a peripheral reactor position in order to alleviate neutronic constraints, a thin salt annulus to achieve thermal design objectives, and high-temperature alloys that provide additional safety margins.

Keywords: Nuclear Reactors, Molten Salt Reactors, Irradiation Testing

1. INTRODUCTION

Idaho National Laboratory is developing a Molten-salt Research Temperature-controlled Irradiation (MRTI) experimental vehicle for the Neutron Radiography (NRAD) reactor. The test vehicle is designed to contain fissile material-bearing chloride salt, which has never before been subjected to a neutron field. To date, similar irradiations have utilized fluoride-based salts [1-4]; however, there is strong interest in using chloride salts for Molten Salt Reactor (MSR) concepts in industry, due to their higher potential actinide content and better suitability for a fast spectrum configuration [5]. The main objectives of the experiment are threefold:

(1) Assess the source term mechanics.
(2) Study the evolution of thermophysical properties with burnup.
(3) Evaluate the impact of irradiation-induced corrosion on materials interfacing with the salt.

A completed conceptual design of this first-of-kind experiment is summarized in this article. A range of parametric analyses were conducted to evaluate different design aspects of the experiment, including the experiment position in NRAD (peripheral or central), structural materials of the vehicle, overall dimensions, and ^{235}U enrichment levels. Suitable design configurations are presented and then compared to each other. The main design constraints include the temperature limits of the salt-facing material, the allowable reactivity margin in the NRAD core, the volume of salt needed for post-irradiation analysis, the salt freezing temperature, and the temperature limits of the NRAD coolant-facing material.

Since maximizing fuel burnup also maximizes the possible scientific outcomes of the experiment, it was prioritized over the other technical requirements. Furthermore, a target fission power density of above 20 W/cm^3 while achieving a target average salt temperature of 600°C was specified as a requirement. This temperature target agrees with MSR design specifications in the literature (e.g., [6-7]). Lastly, the experiment aims to avoid the freezing of salt during reactor operations, due to the risk of radiolysis, which could impact conclusions relating to objective (1). The chosen binary chloride salt, 33%UCl_3-67%NaCl (mole percent), corresponds to the eutectic composition for the compound, maximizing the allowable temperature range for the experiment.

The main design challenge regarding the experiment is to enable fission heat dissipation during neutron irradiation, while simultaneously limiting heat loss during startup, prior to the beginning of reactor operations as the salt should be molten before reactor startup. As a result, an immersion heater design

© 2021 by ASME

was preferred to a furnace-type approach in order to satisfy both requirements. The resistive heater is placed within a thermowell and controls the temperature of the experiment (regardless of whether the reactor is on or off).

A secondary objective of the experiment is to test instrumentation in a high-temperature, salt-interfacing irradiation environment. Four instrumentation positions are envisaged for MRTI. Two will be contained within thermowells to avoid direct contact with the salt. One of the sensors is expected to be a thermocouple (TC) that will monitor the salt temperature. Other instruments under consideration include neutron detectors, needle probes, and pressure gauges.

At least 5 ml of fuel-bearing chloride salt must be recovered for post-irradiation examination (PIE) in order to perform the analyses necessary to achieve the experimental objectives. The experiment will be placed within a NRAD three-pin cluster, with the fourth pin used for the experiment. It will have an open-top fitting so instrumentation cables can be connected to the control system outside the NRAD reactor.

Neutronic simulations of the experiment and its surrounding reactor environment were conducted using the Monte Carlo N-Particle Transport (MCNP) code. Thermal analysis was conducted using ABAQUS finite element software. Mechanical design work focused on generating computer-aided design (CAD) models of the overall MRTI experiment layout and evaluating materials that adhere to applicable codes and standards.

2. DESIGN OVERVIEW AND FUNCTIONAL REQUIREMENTS

2.1 Design Functions and Requirements

The experiment's primary purpose is to irradiate fissile-bearing chloride salt under controlled conditions to achieve the stated objectives. Accomplishing this goal requires a vehicle that can control and monitor irradiation conditions, withstand the harsh environment of a nuclear reactor, contain molten-salt nuclear fuel, and manage the fission heat generated within the salt-fueled capsule. Furthermore, a vehicle unable to easily interface with remote disassembly (hot cell) and PIE facilities would prohibit achieving the scientific outcomes of the sponsoring project. As such, the design team gathered requirements using an interface-based approach. The primary interfaces are listed in Table 1.

TABLE 1: PRIMARY INTERFACES OF THE VEHICLE

Interface	Interface Activity
Researchers	Analyze and publish data obtained from the vehicle and downstream examinations
Test Reactor (NRAD)	Irradiate vehicle
Primary Hot Cell Facility	Remotely disassemble vehicle and remove salt from container
PIE Capabilities	Perform examinations on irradiated materials
Instrument and Equipment Suppliers	Provide commercially available instrumentation and equipment
Fabricators	Fabricate and assemble the vehicle
Transfer Cask	Transfer irradiated vehicle from reactor to primary hot cell facility

Upon completion of the requirements gathering phase, the design team determined several basic required functions for the vehicle:

1. Heat the salt before and during irradiation to maintain a target average temperature
2. Measure the temperature of the salt during irradiation.
3. Contain molten salt and fission products
4. Passively or actively sample gases generated during irradiation
5. Allow remote removal of the irradiated salt

These functions provide context for developing the detailed requirements. The design team identified and documented more than 70 requirements for the vehicle and its connected sub-systems. The bases of these requirements included nuclear and radiological safety, budget limitations, schedule constraints, ensuring the scientific merits of the experiment, etc. Table 2 contains the primary driving requirements for the design. While one requirement shown in the table (the Vehicle-Pool Interface Temperature) confirms that a nuclear safety requirement has been met, the other requirements inform the scientific merit of the design. This requirement subset guided much of the analyses supporting the design during scoping and conceptual design efforts.

TABLE 2: PRIMARY DRIVING REQUIREMENTS OF THE DESIGN

Figure	Characteristic	Value
Burnup	Maximize	N/A
Salt Temperature	Target	600°C
Vehicle-Pool Interface Temperature	Target	70°C
Power Density	Target	20 W/cm^3
Volume of Salt (ml)	Maximize	≥5 ml
Radial and Axial Salt Temperature Gradients	Minimize	N/A
Surface Area-to-Volume Ratio	Minimize	N/A

2.2 Design Scoping and Conceptual Design

The design team considered 11 distinct concepts for the irradiation vehicle. Each concept used different approaches to heat the salt, contain radionuclides, monitor the salt temperature, and insulate the system from the reactor pool. The method of assembly for the different vehicles was also documented. The benefits and drawbacks to each option were also captured in the design process. In some cases, initial calculations were conducted to assess basic feasibility and down-select options.

A major technical outcome of this design phase involved the application of an external heat source for the salt. Often in molten salt experimentation, the salt is heated in a crucible within a furnace. In this case, the thermal energy generated by the heater is transferred radially inwards to the salt, and the furnace is insulated to increase efficiency. At first glance, this concept seems well-suited for the vehicle, given the high target temperature of the salt (600°C) and the low interface temperature between the vehicle and the reactor pool (70°C). However, under neutron irradiation, the fissile-material-bearing salt will generate

© 2021 by ASME

appreciable heat through nuclear fission. This additional heat must be transferred to the reactor pool to prevent temperatures exceeding the structural material limitations. Further complicating the issue is the relatively low assumed thermal conductivity ~0.5 W/mK [8]. Preliminary calculations showed that a furnace-based system was infeasible for the dual role of insulating the salt before reactor startup and dissipating heat during operations. Eliminating all thermal insulation rendered the heater unable to melt the salt while keeping the vehicle-pool interface temperature below 70°C. As a result, four furnace-based design variants were dismissed.

The remaining design options consisted of variations on two basic concepts: (1) an immersion-style heater surrounded by an annulus of molten salt, further contained by two layers of structural material (i.e., austenitic steel or a nickel-chromium superalloy); and (2) a "block" heat transfer monolith using a centrally-located cartridge-style heater with capsules of molten salt placed in different radial positions in the monolith. Both options were further investigated using detailed simulations. Ultimately, the first concept was selected for further parametric analysis. These assessments are the primary emphasis of this article.

3. MECHANICAL DESIGN

The primary mechanical design objective is to maintain safe operating conditions by ensuring the integrity of molten-salt, fission-gas, and inert-gas containment functions. Therefore, the salt-facing material in the inner capsule is fabricated from an ASME Boiler and Pressure Vessel Code (BPVC)-qualified material [9]. Options for this critical salt-containing boundary included austenitic steel type 316L (SS-316L), Inconel 617 (IN-617), and Inconel 625 (IN-625). The MSR community has also shown interest in these alloys for similar reasons [10]. To avoid galvanic effects that would impact corrosion, all salt-facing materials shall use the same alloy composition. Heat management is controlled using an analytically determined mix of inert gases (argon and helium) in a gas-gap configuration that optimizes radial heat transfer from the salt to the reactor coolant water. The gas gap also creates a second containment boundary for the salt in the unlikely event that salt leaks from the inner capsule. All welds in the fabrication and assembly of the vehicle will follow standard company-specific weld procedures. Planned weld inspections include a visual inspection, helium leak check, and dye penetrant examination. Leadouts and thermowells out of the salt-containing inner capsule will be sealed via an induction braze procedure or laser welding. The design will rely on a mechanical Conax®-style connector at the top of the outer capsule to seal the leadouts via compression of a Lava (or roughly equivalent) sealant.

The team identified a cartridge-style immersion heater capable of 800 W output using standard 120 V AC over a ~7.5 cm length and ~1 cm diameter, capable of providing enough heat to melt the salt powder prior to irradiation, as well as maintain temperatures following reactor shutdown to preventing solid salt radiolysis. During the experiment, the heater will also provide supplemental heating to maintain the target temperature. This immersion heater will be inserted into a thermowell to ensure a singular material composition for the inner capsule. The thermowell itself will later provide a material coupon for corrosion studies in PIE. A heat transfer compound paste (T-99 or similar) will ensure dependable contact between the heater and thermowell. Similar smaller thermowells could also be leveraged for select instrumentation, depending on the sheath material and sensor diameter. Instrumentation being considered for the final design include Type N (multi-junction) TCs, self-powered neutron detectors, fiber-optic pressure sensors, and thermal conductivity needle probes. Up to four sensors can be positioned within the molten-salt annulus at once.

3.1 Integration into Existing Reactor Interfaces

Integrating existing interfaces and components into the experiment design was a key strategy in reducing engineering and manufacturing costs. The NRAD TRIGA-type core (Training, Research, Isotopes, General Atomic) features a 6x6 grid plate for fuel clusters, along with surrounding graphite reflectors (shown in Figure 1). The fueled region is the inner 4x4 matrix of clusters. In this core configuration, the two locations of interest for this experiment are the F-1 and C-4 positions, as these locations have been allocated specifically for irradiation experiments in the safety analysis of the core configuration.

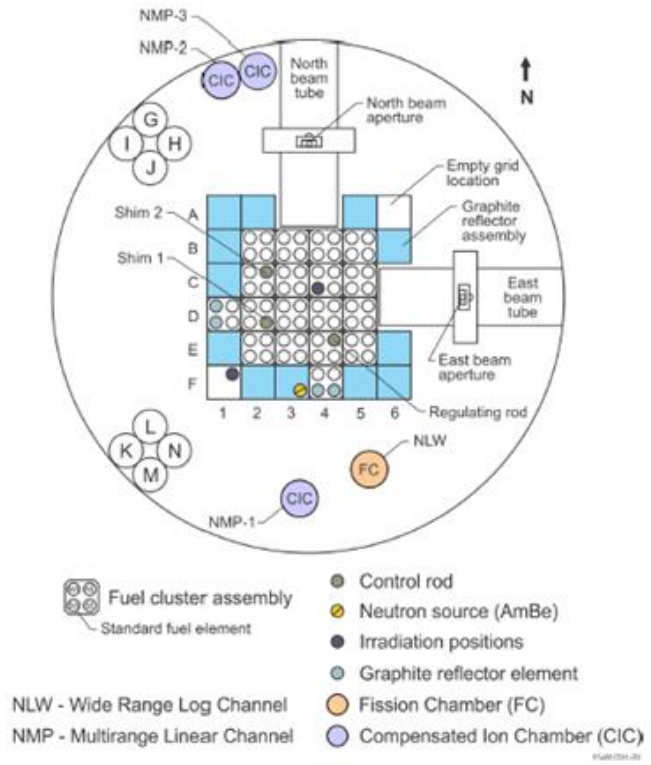

FIGURE 1: NRAD CORE CONFIGURATION AND LAYOUT (TAKEN FROM [11])

Assembly clusters interface into the reactor core via the grid plate, as shown on the right in Figure 2. A bottom cluster end fitting (see the middle illustration in Figure 2) is inserted into a

© 2021 by ASME

grid position and locked from rotation by a pin on the grid plate. This cluster end fitting features four threaded ¾”-10 UNC (Unified National Coarse thread) holes that rod assemblies can be threaded into via the rod end fitting (see the left-hand illustration in Figure 2). Using these three pre-existing components, a design was devised that mimics an element in a traditional bottom cluster end fitting and interfaces directly with the reactor grid plate. The bottom of the experiment outer capsule will feature the same rod end fitting providing a connection to the bottom cluster end fitting.

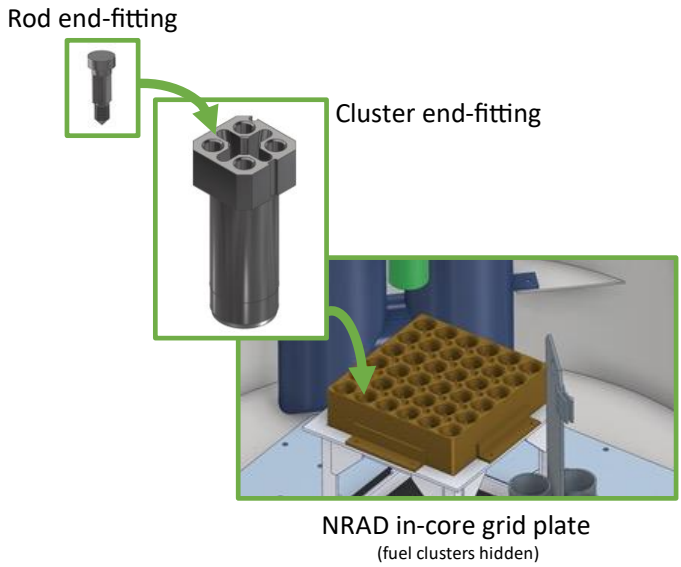

FIGURE 2: ASSEMBLY OF A PIN INSIDE A CLUSTER WITHIN THE NRAD GRID PLATE

Due to the space requirements of the experiment capsule design—predominately arising from the need for a mechanical Conax® seal gland—it was determined that the preferred cluster configuration would be similar to the wet guide tube design already existing within the reactor’s C-4 position (see Figure 3). The key benefit of this design—a benefit unavailable with the standard fuel cluster—is that this configuration allows one element to extend beyond the handle. This feature would enable, from an electrical wiring standpoint, greater versatility in the design. This three-pin cluster configuration uses a 45° top bail assembly that varies from the traditional fuel-cluster top bail but uses the same locking plate and bolt design to secure the cluster in place. To interface with this top bail, the experiment outer capsule must match the typical ~4 cm outer diameter of the C-4 wet tube at this top section using an additional fitting component. The final experiment assembly can be seen on the right-hand side in Figure 3, with the other three cluster positions being filled by Al6061-T6 surrogate rods to maintain the structural integrity of the cluster while avoiding major neutronic penalties.

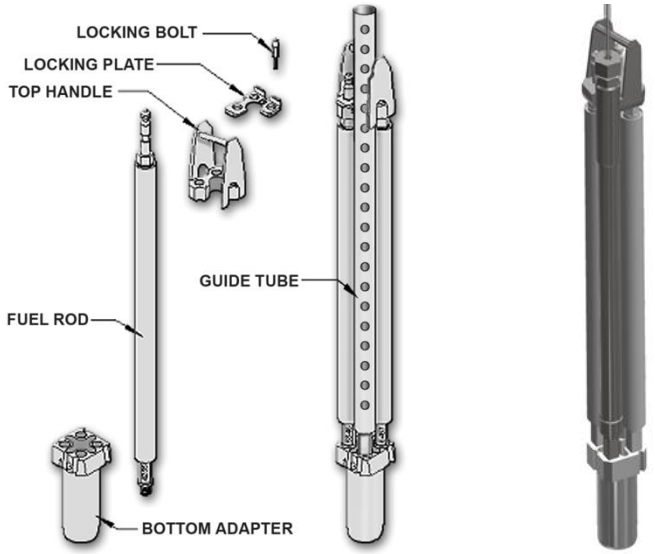

FIGURE 3: EXISTING NRAD WET GUIDE TUBE CLUSTER (LEFT) [11] AND RESULTING MRTI CONCEPT (RIGHT)

3.2 Conceptual Design

The conceptual design was developed following iterative modeling and analysis for neutronics and thermal performance, as discussed in Sections 5 and 6, respectively. The inner salt-containing capsule is placed within the outer containment. To center the salt at core midplane, a graphite reflector is used to raise the capsule to the desired height, in addition to providing some neutron reflection. Similarly, graphite reflectors were placed over the top of the inner capsule. Note that the top reflectors will be cut and drilled into quadrant sections to provide adequate spacing for instrumentation and heater leadouts. An alumina insulating wafer is placed directly below the capsule to reduce the axial thermal conduction into the bottom graphite reflector.

The inner capsule geometry strongly depends on structural, neutronic, and thermal considerations. For example, Inconel allows for a larger thermal gradient compared to SS-316. Inconel alloys can maintain integrity at temperatures approaching 800–1000°C. The salt annulus inside the capsule will be approximately 7 cm in height, with a thickness of 0.3–0.5 cm. Instrumentation will be uniformly spaced within this annulus of molten salt. At the center of the capsule, the cartridge immersion heater will have an active heating height of around ~7.5 cm. To ensure the integrity of the heater leadout junction, which is made from a high-temperature epoxy on a slight swage, the heater features an additional unheated section of ~12 cm. This positions the junction above the top of the inner capsule, greatly reducing its operating temperature. The gas gap for design variations is around ~0.08 cm. This thickness provides sufficient insulation between the inner and outer capsule, as well as enough space to alleviate potential thermal expansion. The gap will be maintained via two three-pronged sections of standoff geometries that will concentrically hold in place the inner capsule within the outer can.

© 2021 by ASME

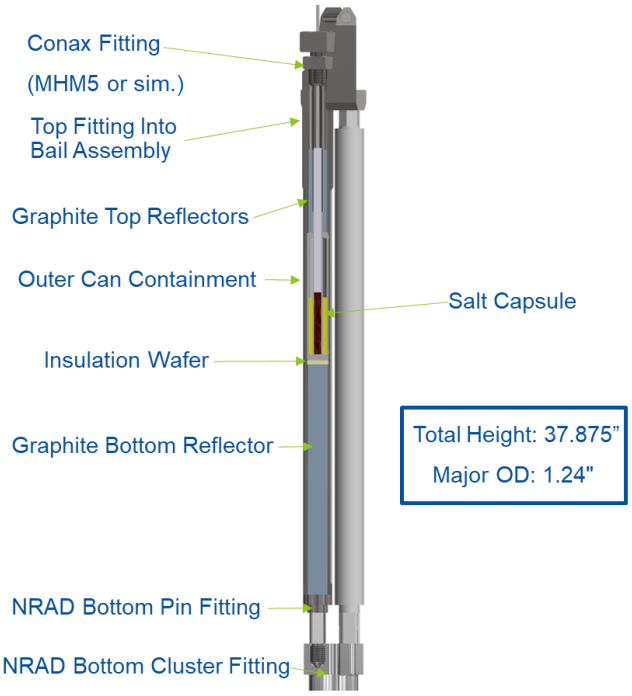

FIGURE 4: OVERVIEW OF THE MRTI CLUSTER CAD MODEL

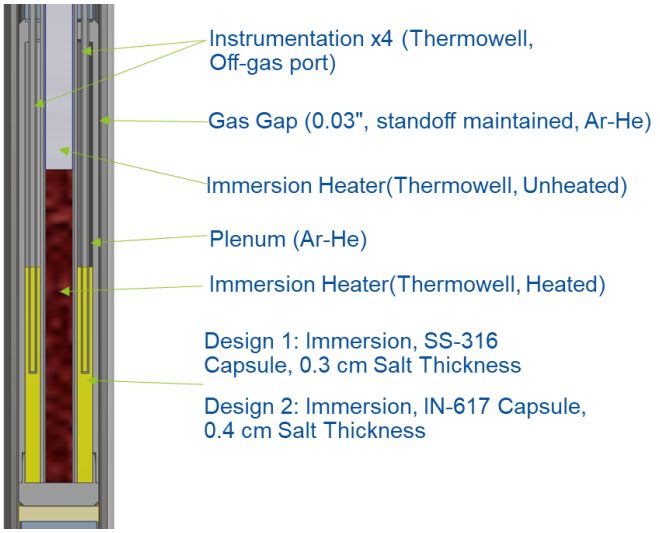

FIGURE 5: CROSS-SECTIONAL VIEW OF THE INNER CAPSULE CAD MODEL

4. CONTROL SYSTEM

The primary objective of the control system is to maintain the target salt temperature for the duration of the experiment. Careful design considerations are expected to be the key drivers of the temperature distribution throughout the experiment. Nevertheless, a control system will be needed to correct for potential uncertainties and deviations from expected operations.

The desired operating sequence consists of five basic steps: (1) heat the salt to the target temperature and hold it there until thermal equilibrium is reached; (2) as the reactor powers up, continue to maintain the temperature by decreasing the heater power to compensate for the added heat from fission energy release; (3) continue to maintain the temperature during reactor steady-state operation; (4) as the reactor powers down, continue to maintain temperature by inversely increasing the heater power; and finally, (5) continue to maintain the salt temperature following reactor shutdown, until the experiment is ready for transport and examination.

Figure 5 is a block diagram of the physical layout of the major control components, showing interfaces to the heater and instrumentation. A standard Allen-Bradley CompactLogix controller is proposed for controlling the heater, with a sample rate of around 1 Hz. TC feedback for heater control can be based on a specific TC or the average of several. Heater cycling will be minimized by implementing a solid-state control relay utilizing zero-cross voltage control. A separate independent controller will provide over-temperature shutdown during unanticipated excursions.

System control and monitoring will be performed through human-machine interface (HMI) touchscreens/keyboards in the NRAD control room. An independent heater shutdown switch will also be provided. In addition to allowing for the input of variables such as target temperature, the HMI screens will provide real-time instrumentation output, trending, and system performance data.

Software will be utilized in parallel with the controller and HMI to provide at least seven days of onboard data storage. A separate facility data acquisition system is available for continuous data collection once an experiment is connected.

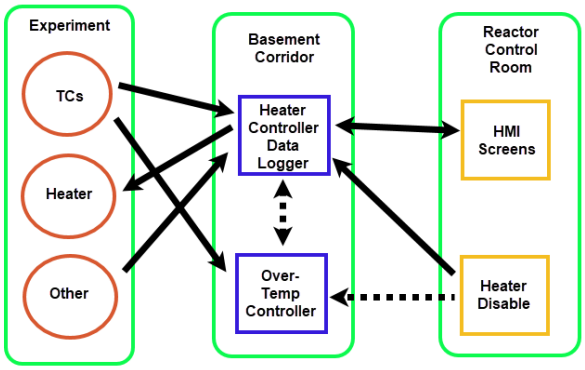

FIGURE 6: MRTI EXPERIMENT CONTROL BLOCK DIAGRAM

5. NEUTRONIC ANALYSIS

5.1 Model Development

The neutron transport code MCNP6.1 was used for the neutronic analysis [12]. A representative model of the NRAD core geometry was used for this purpose, with the experiment explicitly modeled within the core geometry, as shown in Figures 7 and 8. While limited data exist on the UCl_3-NaCl salt considered here, information on the density of this compound as a function of temperature was found in [13].

© 2021 by ASME

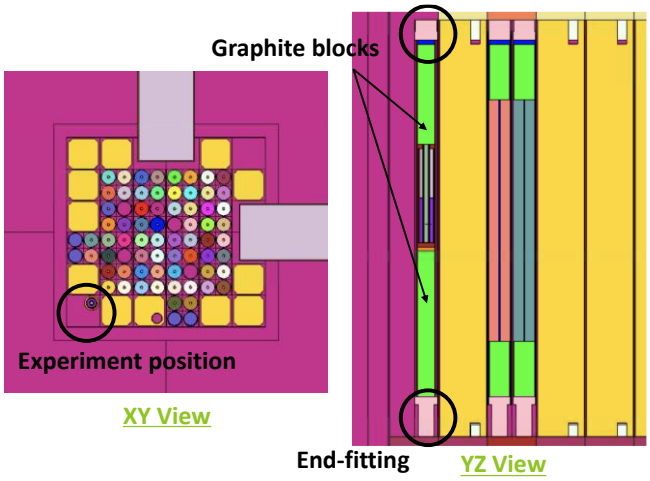

FIGURE 7: VISUALIZATION OF THE MRTI EXPERIMENT INSIDE THE NRAD CORE

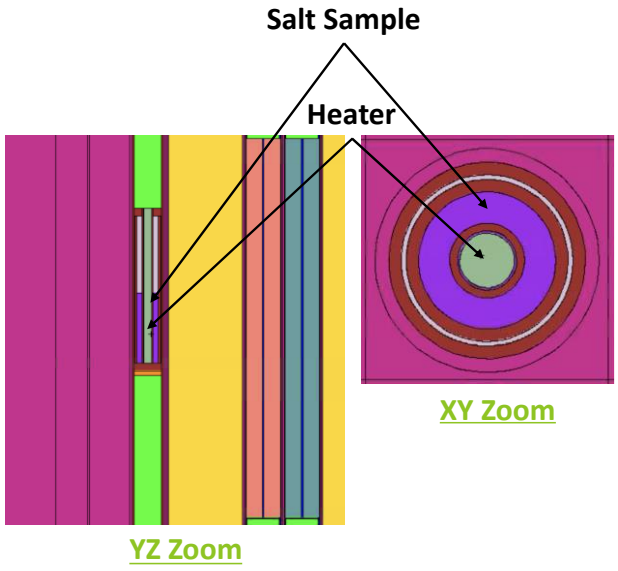

FIGURE 8: ZOOMED-IN VIEW OF THE MRTI EXPERIMENT MODEL IN MCNP

A total of 100,000 virtual particles were used, with 1,000 cycles per simulation (100 of which were inactive). This ensured that the Monte Carlo eigenvalue standard deviations were kept below 10 pcm. Similarly, the average standard deviation in the MRTI flux tallies was 0.5%. Both neutron and gamma particles were modeled in order to adequately account for radiation heating effects within the experiment.

The primary design considerations for the neutronic analysis are the fission heat generated within the salt, heat generation within the different experiment components, and the reactivity margin caused by insertion of the experiment. Energy deposition tallies were used to assess the first two items, while direct perturbation was used to estimate the impact on reactivity.

The main design considerations are summarized in the design matrix in Table 3. Two NRAD positions were investigated: F-1 (shown in Figure 7) and C-4 (in the center of the core). A range of materials were considered for the inner and outer capsule. Different salt thicknesses were also investigated; decreasing the salt thickness reduces thermal gradients but would complicate salt removal during PIE activities. Two uranium enrichments were also considered: 19.75wt% ^{235}U high-assay low-enriched uranium (HALEU) and ~93wt% ^{235}U highly enriched uranium (HEU).

TABLE 3: EXPERIMENT DESIGN MATRIX OPTIONS AND CONSIDERATIONS

Variable	Options	Considerations
Outer can	Al/SS-316/IN-617	Temperature and manufacturing
Inner capsule	SS-316/IN-617	Temperature and corrosion
NRAD position	F-1/C-4	Power density and temperature
Salt thickness	0.3/0.4/0.5 cm	PIE and temperature
^{235}U enrichment	19.75 wt% / 93 wt%	Power density and temperature

5.2 Heat Generation Rates

A parametric evaluation was conducted to assess the power density for different design considerations. The initial results are summarized in Tables 4 and 5. Overall, it was found that:

- Salt with HALEU enrichment cannot reach the power density target in either F-1 or C-4.
- The power density takes a minor penalty from using SS-316L as the outer can material instead of Al.
- Transferring the experiment to the C-4 position can contribute to a 2× increase in fission power.
- Using IN-617 as the inner capsule material contributes to a ~17% drop in power density.
- Using IN-617 for both the capsule and outer can contributes to a more significant ~30% drop and is therefore discouraged.
- Each 0.1 cm in salt thickness reduction contributes to an approximately 10 W/cm^3 increase in average power density.

TABLE 4: IMPACT OF OUTER CAN, NRAD POSITION, AND SALT ENRICHMENT ON SALT FISSION POWER DENSITY

Outer can	Al	Al	Al	SS-316	SS-316
Inner capsule	SS-316	SS-316	SS-316	SS-316	SS-316
NRAD position	F-1	C-4	F-1	F-1	C-4
Salt thickness	0.5 cm	0.5 cm	0.5 cm	0.5 cm	0.5 cm
^{235}U enrichment	19.75 wt%	19.75 wt%	93 wt%	93 wt%	93 wt%
Salt volume	18.7 ml	18.7 ml	18.7 ml	18.7 ml	18.7 ml
Flux in salt	3.47 × 10^{12} n/cm^2-s	1.61 × 10^{13} n/cm^2-s	4.43 × 10^{12} n/cm^2-s	4.00 × 10^{12} n/cm^2-s	1.72 × 10^{13} n/cm^2-s
Fission power	8.78 W/cm^3	13.09 W/cm^3	29.07 W/cm^3	24.63 W/cm^3	49.10 W/cm^3

© 2021 by ASME

TABLE 5: IMPACT OF OUTER CAN, INNER CAPSULE, AND SALT THICKNESS ON SALT FISSION POWER DENSITY

Outer can	SS-316	IN-617	SS-316	SS-316	SS-316
Inner capsule	SS-316	IN-617	IN-617	IN-617	IN-617
NRAD position	F-1	F-1	F-1	F-1	F-1
Salt thickness	0.3 cm	0.5 cm	0.5 cm	0.4 cm	0.3 cm
^{235}U enrichment	93 wt%	93 wt%	93 wt%	93 wt%	93 wt%
Salt volume	9.9 ml	18.7 ml	18.7 ml	14.1 ml	9.9 ml
Flux in salt	4.12×10^{12} n/cm^2-s	3.27×10^{12} n/cm^2-s	3.60×10^{12} n/cm^2-s	3.64×10^{12} n/cm^2-s	3.68×10^{13} n/cm^2-s
Fission power	35.73 W/cm^3	17.08 W/cm^3	20.39 W/cm^3	23.99 W/cm^3	29.15 W/cm^3

5.3 Reactivity Margin

The absolute reactivity insertion from the experiment must be maintained within NRAD safety margins of $\pm$ 40 cents. The reactivity of different experimental configurations relative to the base NRAD model (with the experiment position filled with water) is shown in Table 6. Overall, it was found to be prohibitively challenging to place the experiment in C-4 while still satisfying the reactivity margin constraints. Different MRTI axial reflector materials can help alleviate the concern but cannot sufficiently reduce the absolute value of reactivity change. Through perturbation analysis, it was determined that simply voiding the water in the C-4 channels already contributes to a -67 cents reactivity penalty. Consequently, it is challenging for the experiment to contribute a net increase of greater than +27 cents to compensate for the inevitable water displacement.

TABLE 6: REACTIVITY CONSIDERATIONS IN THE DESIGN OPTIMIZATION. ALL CASES INVOLVE SS-316 AS BOTH THE INNER AND OUTER CAPSULE/CAN MATERIAL, A URANIUM ENRICHMENT OF 93%, AND A SALT THICKNESS OF 0.5 CM

NRAD position	C-4	F-1	C-4	C-4	C-4
Salt height	7 cm	7 cm	7 cm	7 cm	10 cm
Axial reflector	Graphite	Graphite	$ZrH_{1.6}$	BeO	Graphite
Salt volume	18.7 ml	18.7 ml	18.7 ml	18.7 ml	26.7 ml
Reactivity	-56.5 cents	+1.86 cents	-54.8 cents	-47.5 cents	-49.3 cents

The main concern with the negative reactivity margin relates to Xe preclusion: a large penalty could complicate the NRAD reactor restart time. This could be alleviated by reducing the overall power of the reactor. Since experiment configurations in C-4 have adequate margins in regard to fission power, this may be acceptable. Ultimately, however, opting for the F-1 position in NRAD is still recommended for facilitating mechanical design (larger volume) and reactor operations.

5.4 Heat Generation Rates for Thermal Analysis

For the purposes of the heat transfer analysis in Section 6, heat generation values across different layers of interest must be captured. The heat contributions of the different experiment layers are summarized in Table 7 for two primary design variants that were investigated further. Note that the salt heating values do not correspond to those in Tables 4 and 5, since the fission heating source does not always account for gamma energy deposition outside the salt.

TABLE 7: HEAT GENERATION IN DIFFERENT PARTS OF THE EXPERIMENT (BOTH CASES ARE IN THE F-1 POSITION AND RELY ON HEU FUEL)

Capsule material	SS-316	IN-617
Salt thickness	0.3 cm	0.4 cm
Average Heat Generation (W/cm^3):		
Salt	33.698	33.698
Resistive heater and sheath	22.693	22.693
Capsule radial wall	0.160	0.160
Outer can radial wall	0.172	0.172
Lower graphite reflector	0.217	0.217
Insulating disk	0.254	0.254
Capsule lower wall	0.142	0.142
Capsule upper wall	0.142	0.142
Upper graphite reflector	0.024	0.024

6. THERMAL ANALYSIS

6.1 Model Development

The finite element analysis software ABAQUS 6.14-2 [14] was used to develop an axisymmetric model for the thermal analysis. Although it is possible for natural convection to develop within a pool of salt, the UCl_3-NaCl annulus was treated as stagnant. The impact of natural circulation is expected to be minimal. The thermal analysis was simplified such that specific models were not generated for the various combinations of experiment features pertinent to the thermal analysis. A parametric scoping study was performed using salt thickness, insulating gas, and heater operation.

6.2 Salt Thickness Scoping Study

Various thicknesses of the salt annulus were proposed. Thinner salt annuli generate smaller temperature gradients but are expected to be more difficult to remove for PIE. The thicker salt annuli generate larger temperature gradients that could challenge temperature limits but would be easier to remove for PIE.

The thickness-dependent temperature gradients are shown in Figure 9, with Node 1 being the closest to the heater and Node 4 being the closest to the inner capsule wall along the horizontal plane—where the maximum salt temperature is reached. Based on the need for balancing the temperature

© 2021 by ASME

gradient and for ease of salt removal, annuli thicknesses of 0.3 and 0.4 cm were chosen for parametric studies.

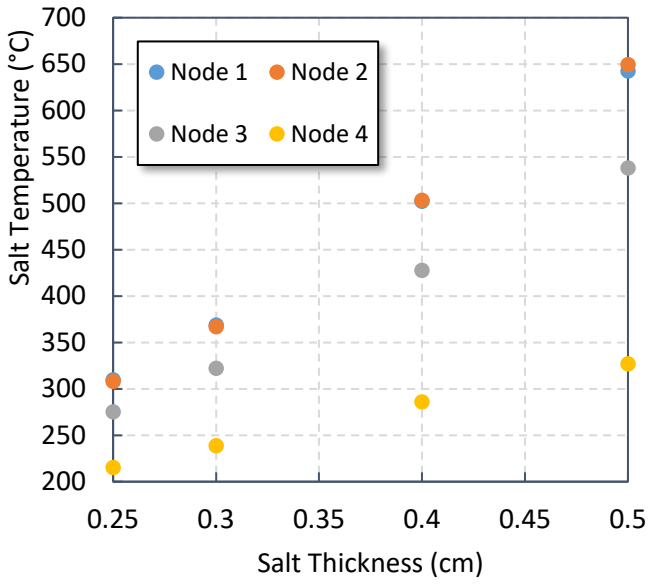

FIGURE 9: RESULTS OF PARAMETRIC STUDY ON SALT ANNULI THICKNESS

6.3 Thermal Bounding Analysis

Parametric studies on the insulating gas and heater operation were performed for both salt annulus thicknesses. Since the insulating gas will be a mixture of helium and argon, cases with pure helium and pure argon were analyzed to determine the minimum and maximum salt temperatures as well as the expected salt temperature gradients. This provides bounding cases for the analysis.

The results presented in this subsection are for a radial planar cross section of the experiment, corresponding to the point where the highest temperatures were observed. To isolate the impact of the heater operation, the heat input to the experiment was either purely a result of the fission heat generation rate provided from the neutronic analysis or solely that of the heater output.

The results of this combined parametric study are shown in Figures 10 and 11. Cases with only fission heat had similar gradients, but argon, given its lower thermal conductivity, led to cases with maximum temperatures exceeding the target values. When the heater is the only heat source, a pure helium gas gap results in an undesirable temperature gradient, while a pure argon gas gap can achieve the target salt temperature. Therefore, a mixture of the two gases is expected to satisfy the experiment temperature requirements. The exact composition will be determined as part of the final design analysis.

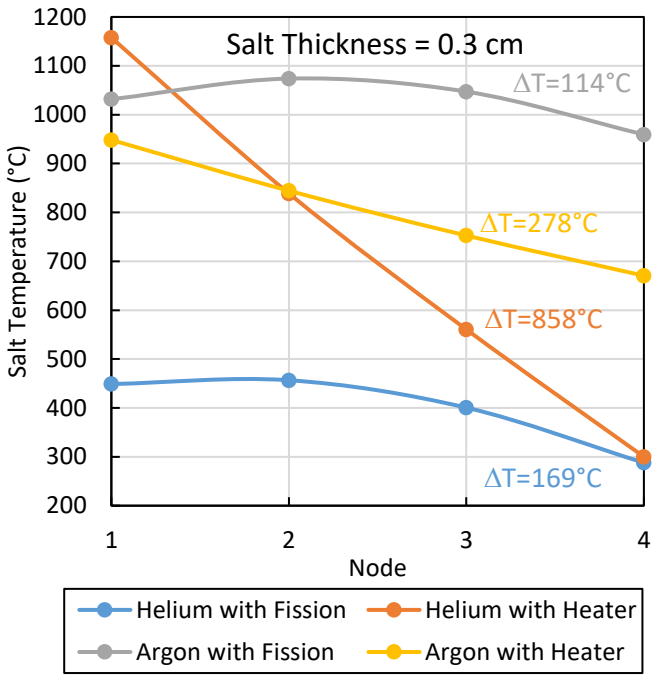

FIGURE 10: RESULTS OF PARAMETRIC STUDY ON INSULATING GAS AND HEATER OPERATION FOR 0.3 CM SALT; NOTE THAT THE DISTRIBUTIONS ARE AT DIFFERENT AXIAL PLANES BETWEEN EACH CASE

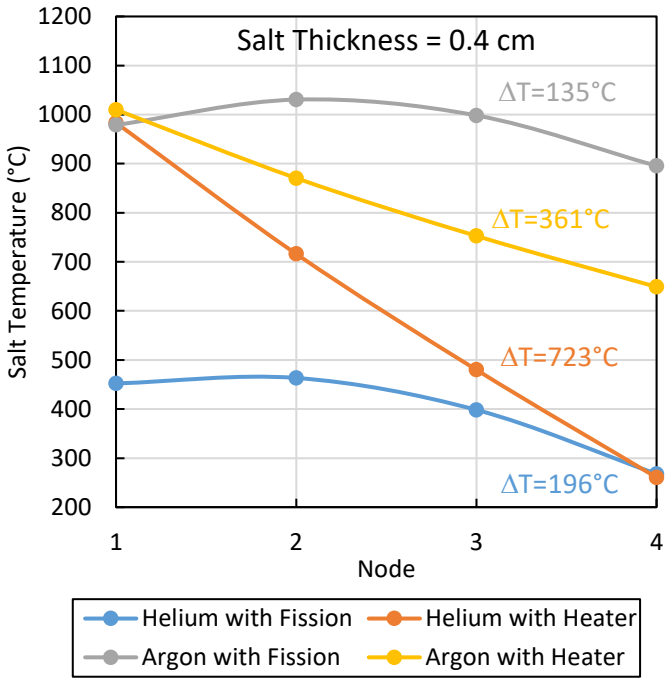

FIGURE 11: RESULTS OF PARAMETRIC STUDY ON INSULATING GAS AND HEATER OPERATION FOR 0.4 CM SALT; NOTE THAT THE DISTRIBUTIONS ARE AT DIFFERENT AXIAL PLANES BETWEEN EACH CASE

© 2021 by ASME

The capsule material was another design option considered in previous evaluations. Here, the selection of IN-617 versus SS-316 was found to have a negligible impact on the overall temperature distribution within the system. Nevertheless, IN-617 can withstand higher temperatures while maintaining structural integrity. IN-617 was therefore recommended for the final design in order to provide adequate margins.

6.4 Overall Experiment Thermal Performance

ABAQUS heat transfer simulations were also used to determine if the high target temperature of the salt (600°C) and low interface temperature between the vehicle and reactor pool (70°C) could be met. The previous configurations introduced in Section 6.3 were evaluated, with axial variations taken into consideration when determining bounding conditions. The main purpose was to quantify the minimum, maximum, and average salt temperatures, as well as the maximum experiment-pool interface temperatures.

For all of the cases considered (i.e., heater on/off, Ar versus He, etc.), similar 2-D temperature distribution patterns were observed, leading to predictability in locations of minimum and maximum salt temperatures. A unitless representation of the salt temperature distributions is provided in Figure 12. Note that red indicates the highest temperatures, while blue indicates the lowest. As expected, temperature is at a maximum near the center of the salt when only accounting for fission heat. On the other hand, a more radial distribution is observed when only accounting for the heater output. The temperature is higher at the top of the capsule, due to plenum gas insulation. In reality, a combination of both distributions is expected, as a certain amount of heater power will be required to supplement fission heating.

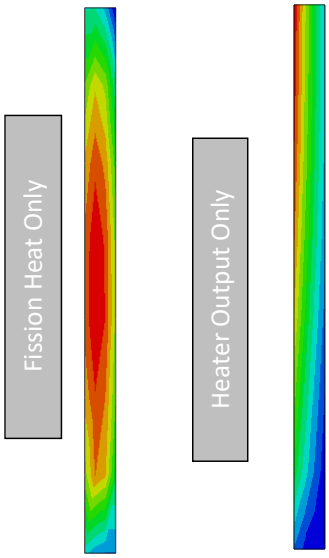

FIGURE 12: UNITLESS R-Z AXISYMMETRIC REPRESENTATIVE SALT TEMPERATURE DISTRUBTION WITH FISSION OR HEATER OUTPUT ONLY

The results of the heat transfer simulations are reported in Tables 8 and 9. Helium does not insulate as effectively as argon, thus the minimum temperatures associated with a gas gap of pure helium were significantly lower than those associated with a gas gap of pure argon. Pure helium also resulted in a more pronounced temperature gradient when relying solely on the heater instead of only on fission heat. The vehicle-pool interface temperatures were at maximum when a pure helium gas gap was analyzed, with only one case violating the vehicle-coolant interface temperature limit.

TABLE 8: IMPORTANT TEMPERATURE METRICS FOR 0.3 CM SALT

Gas	Fission/ Heater	Salt T_{min} (°C)	Salt ΔT (°C)	Interface T_{max} (°C)
He	On/Off	192	264	69
He	Off/On	260	898	72
Ar	On/Off	712	362	62
Ar	Off/On	553	396	54

TABLE 9: IMPORTANT TEMPERATURE METRICS FOR 0.4 CM SALT

Gas	Fission/ Heater	Salt T_{min} (°C)	Salt ΔT (°C)	Interface T_{max} (°C)
He	On/Off	178	286	67
He	Off/On	228	756	67
Ar	On/Off	657	374	61
Ar	Off/On	543	467	54

The heat transfer simulation results indicate that the salt target temperature and vehicle-pool interface temperature requirements can be met. As with the parametric scoping study, the actual temperatures will depend on the final mixture of helium and argon used in the gas gap.

7. FUTURE WORK

The design is expected to continue to evolve over the near term. Before finalizing specifications, multiple prototyping and mock-up activities will be conducted to test remote salt removal abilities, material joining techniques, and system integration, as well as to validate heat transfer models. The neutronic and thermal analyses will be updated to account for self-shielding effect in the salt power distribution. A 3-D power distribution will be provided to ABAQUS to more accurately represent variations in heat generation within the annulus. Computational fluid dynamics (CFD) simulations will be performed to confirm the accuracy of natural-circulation assumptions. Upon completing the final design and experiment safety reviews, fabrication of the experiment can commence, with irradiation in NRAD planned for calendar year 2022.

8. CONCLUSION

Parametric scoping studies were performed on a fuel-bearing salt irradiation experiment for the NRAD reactor. Analysis included neutron transport simulation, finite element

© 2021 by ASME

heat transfer analysis, and a detailed CAD evaluation. A range of different materials, reactor positions, salt thicknesses, and fuel enrichments were considered. Ultimately, the analysis concluded that a double-encapsulated system with an immersion heater arrangement, a 0.4 cm salt annulus, HEU fuel, and IN-617 capsule material could achieve the design objectives of the experiment.

ACKNOWLEDGEMENTS

This research work was prepared for the U.S. Department of Energy through the INL LDRD program, grant number 21A1050-016FP, under the DOE Idaho Operations Office. It also made use of INL's high-performance computing resources. Contract No. DE-AC07-05ID14517.

The United States Government retains, and by accepting the article for publication, the publisher acknowledges that the United States Government retains, a non-exclusive, paid-up, irrevocable, worldwide license to publish or reproduce the published form of this work, or allow others to do so, for United States Government purposes.

REFERENCES

[1] Jordan, W. H., S. J. Cramer, and A. J. Miller. "Aircraft Nuclear Propulsion Program: Quarterly Progress Report for Period Ending December 31, 1956." Technical Report ORNL-2221, Oak Ridge National Laboratory, Oak Ridge, TN. 1957. https://doi.org/10.2172/1373535.

[2] Savage, H. C., E. Compere, J. M. Baker, and E. G. Bohlmann. "Operation of Molten-Salt Convection Loops in the ORR." Technical Report ORNL-TM-1960, Oak Ridge National Laboratory, Oak Ridge, TN. 1960. https://doi.org/10.2172/4580057.

[3] Trauger, D. B. and J. A. Conlin Jr. "Circulating Fused-Salt Fuel Irradiation Test Loop." *Nuclear Science and Engineering* Vol. 9 No. 3 (1961): pp. 346–356. https://doi.org/10.13182/NSE61-A25886.

[4] Kedl, R. J. "The Migration of a Class of Fission Products (Noble Metals) in the Molten-Salt Reactor Experiment." Technical Report ORNL-TM-3884, Oak Ridge National Laboratory, Oak Ridge, TN. 1972. https://doi.org/10.2172/4471292.

[5] Seo, S. B., Y. Shin, and I. C. Bang. "Review on the current status of molten chloride reactor and its future prospect." *Transactions of the Korean Nuclear Society Autumn Meeting*, Gyeongju, Korea, October 27–28, 2016.

[6] Mourogov, A. and P. M. Bokov. "Potentialities of the fast spectrum molten salt reactor concept: REBUS-3700." *Energy Conversion and Management* Vol. 47 No. 17 (2006): pp. 2761–2771. https://doi.org/10.1016/j.enconman.2006.02.013.

[7] Altahhan, M. et al., "3D Coupled Transient simulation of a Fast Liquid Fuel Molten Salt Reactor Primary Loop Using GeN-Foam." *Proceedings of NURETH-18*, Portland, OR, August 18–22, 2019.

[8] Bystrai, G. P., V. N. Desyatnik, and V. A. Zlokazov. "Thermal conductivity of molten mixtures of uranium tetrachloride with sodium and potassium chlorides." *Soviet Atomic Energy* Vol. 36 (1974): pp. 654–655. https://doi.org/10.1007/BF01127242.

[9] American Society of Mechanical Engineers. *ASME Boiler and Pressure Vessel Code (BPVC).* ASME, New York (2019).

[10] Electric Power Research Institute. "Program on Technology Innovation: Material Property Assessment and Data Gap Analysis for the Prospective Materials for Molten Salt Reactors: Research and Development." Technical Report ID-3002010726, EPRI, Palo Alto, CA. 2019.

[11] Bess, J. D., J. B. Higgs, and R. M. Lell. "Neutron Radiography (NRAD) Reactor 64-Element Core Upgrade." Technical Report INL/EXT-13-29628, Idaho National Laboratory, Idaho Falls, ID. 2014. https://doi.org/10.2172/1120810.

[12] Pelowitz, D., T. Goorley, and M. James. "MCNP6 User's Manual, v1.0." LA-CP-13-00634, Los Alamos National Laboratory, Los Alamos, NM. 2013.

[13] V. N. Desyatnik, V. N, Katyshev, S. F., Raspopin, S. P. and Chervinskii, Y. F. "Density, Surface Tension, and Viscosity of Uranium Trichloride-Sodium Chloride Melts." *Atommaya Energiya* Vol. 39 (1975): pp. 70–72.

[14] ABAQUS Standard, Version 6.14-2, SIMULIA, Inc., Providence, RI. 2014.

 © 2021 by ASME